TEXTURE EVOLUTION VIA CONTINUOUS TIME RANDOM WALK THEORY

M. EMELIANENKO*, D. GOLOVATY†, D. KINDERLEHRER‡, AND S. TA'ASAN§

Abstract.
Under standard processing conditions, many materials possess polycrystalline microstructures composed of a large number of small monocrystalline grains separated by grain boundaries. The energetics and connectivity of the grain boundaries network plays a crucial role in defining the properties of a material across a wide range of scales. A central problem in materials science is to develop technologies capable of producing arrangements of grains—textures—that provide for a desired set of material properties.

One of the most challenging aspects of this problem is to understand the role of topological reconfigurations during coarsening. In this paper, we study mesoscopic behavior of a one-dimensional grain boundary system and investigate the possibility of modeling texture evolution. We suggest a stochastic framework based on the theory of continuous time random walks that may be used to model this system. We compare the predictions of the corresponding evolution equations with simulations and discuss their limitations and possible extensions to higher-dimensional cases.

1. Introduction. Most technologically useful materials arise as polycrystalline microstructures, composed of myriads of small crystallites, called grains, separated by interfaces, called grain boundaries. The energetics and connectivity of the network of boundaries are implicated in many properties across wide scales, for example, functional properties, like conductivity in microprocessors, and lifetime properties, like fracture toughness in structures. Preparing arrangements of grains and boundaries suitable for a given purpose is a central problem in materials science. It likewise presents many challenges for mathematical modeling, simulation, and analysis. Historical emphasis here has been on the geometry, or more exactly, on statistics of simple geometric features of experimental and simulated polycrystalline networks. We are now turning our attention to texture, the mesoscopic description of arrangement and properties of the network described in terms of both geometry and crystallography.

There is a great wealth of experimental work available concerning texture in polycrystalline systems: it has, after all been of recognized importance since the stone age (see [1]) In recent years, we have witnessed a changing paradigm in the materials laboratory with the introduction of automated data acquisition technologies. This has permitted the collection of statistics on a vast scale and its use to optimize aspects of material behavior. There are situations, for example, where it is possible to quantify the amount of alignment or misalignment sufficient to produce a corrosion resistant microstructure. To rise beyond this level of anecdotal observation, the thermodynamics of the material system must be related to texture and texture related properties. Said in a different way, are there any texture related distributions which are material properties? Some geometric features of the configuration, like relative area statistics have these properties in the sense that they are robust but they are not strongly related to energetics. Recent work has provided us with a new statistic, the

*Department of Mathematical Sciences, Carnegie Mellon University, Pittsburgh, PA 15213 email: masha@cmu.edu.

† Department of Theoretical and Applied Mathematics, The University of Akron, Akron, OH 44325, email: dmitry@math.uakron.edu.

‡ Department of Mathematical Sciences, Carnegie Mellon University, Pittsburgh, PA 15213, email: davidk@cmu.edu.

§ Department of Mathematical Sciences, Carnegie Mellon University, Pittsburgh, PA 15213, email: shlomo@andrew.cmu.edu.

grain boundary character distribution, which has enormous promise in this direction. The grain boundary character distribution is a measure of relative amount of grain boundaries with a given net misorientation. Owing to our new ability to simulate the evolution of large scale systems, we have been able to show that this statistic is robust and, in elementary cases, easily correlated to the grain boundary energy [2], [3], [4].

We stress, however, that the mechanisms by which the distribution develops from an initial population are not yet understood. As a polycrystalline configuration coarsens, facets are interchanged and some grains grow larger and others disappear. These critical events determine the evolution of our distribution. This is because the system coarsens by the motion of the triple junctions, with low energy boundaries sweeping out those of higher energy. The triple junction population, in turn, is determined by the critical events. The regular evolution of the network is governed by the Mullins equations of curvature driven growth supplemented by the Herring condition force balance at triple junctions, a system of parabolic equations with complementing boundary conditions (see [5],[6]). The critical events, on the other hand, are stochastic.

The major difficulty in developing a theory of the grain boundary character distribution lies in the lack of understanding of these stochastic events. In this work we concentrate our effort on the mechanisms governing these processes. Here we shall investigate a simplified 1-dimensional model that serves as a surrogate, exhibiting the main features of the interacting grain boundary network. In this model, we shall have boundaries and junctions between boundaries moving under a form of gradient flow. It is introduced precisely in the Section 2.2.

There are several approaches one might adopt to describe the behavior of the grain boundary character density, from purely deterministic to stochastic. Motivated by the apparent presence of stationary distributions coming out of the statistical analysis of such a system as described in Chapter 5.1, we consider theoretical frameworks capable of describing it. For example, one possible such framework based on statistical mechanics is introduced in [7], where we construct a Boltzmann-type equation modeling grain interaction which can successfully reproduce simulation data in long time scale with the adequate choice of parameters and has a good potential for generalization to higher dimension. In fact, it appears that this approach can yield even better results in 2D due to the the restrictions that 1-dimensional problem poses on grain interactions, in contrast to its visual simplicity. Here we focus our attention on the strategy we found to be most promising. In Chapter 3.1 we look at the traditional continuous time random walk (CTRW) theory, which turned out to be the most flexible way to handle the complexity observed in this type of jump process. In addition to the "intuitive" random walk derivation, we provide an alternative way to derive the master equation for the most general random walk, relying exclusively on probabilistic tools. We conjecture the fractional nature of the grain boundary kinetics and propose unified approach to model it in terms of generalized fractional master equations. We test our theoretical ideas on a 1-dimensional problem designed specifically to target critical events evolution observed in microstructure. In Chapter 5, we identify the set of stable statistics and confirm the subdiffusive nature of the underlying kinetics. Finally, in 5.2 we compare the statistics obtained by direct simulation with the results of the generalized master equation developed through CTRW theory.

The purpose of this paper is to propose a set of tools that can be used to model the evolution of critical events in microstructure. Without aiming to obtain a unique solution to the problem, we describe a theory that has a potential for successfully

describing each stage of the grain growth dynamics in the higher dimensional systems.

2. Simplified model description. Our principal goal is to understand whether it is possible to derive a stochastic model of grain growth by conducting numerical experiments for a large number of evolving grains, collecting the appropriate statistical data, and using this data to formulate a mathematical model governing the evolution of relevant effective characteristics. In this paper, we demonstrate the feasibility of this approach by considering a "toy" one-dimensional system of grain boundaries represented by intervals on a number line. Note that we do not claim that such a system is physically realistic—there is no curvature-driven propagation in one dimension. Rather, our interest is in studying the dynamics of a system where interactions between grain boundaries resemble qualitatively those observed in a real polycrystalline material. We assume that each grain boundary is described by its length and a prescribed "orientation". We require that there are only nearest-neighbor interactions between the grain boundaries and that the strength of the interactions depends on values of the orientation parameter for the neighboring boundaries.

To make our construction precise, fix $L > 0$ and consider the intervals $[x_i, x_{i+1}]$, $i = 0, \dots, n-1$ on the real line where $x_i \leq x_{i+1},\ i = 0, \dots, n-1$ and $x_n = x_0 + L$. The locations of the endpoints $x_i,\ i = 0, \dots, n$ may vary in time however the total length L of all intervals remains fixed. For each interval $[x_i, x_{i+1}]$, $i = 0, \dots, n-1$, choose a number α_i from the set $\{\alpha_j\}_{j=1,\dots,n}$. The intervals $[x_i, x_{i+1}]$ correspond to grain boundaries and the points x_i represent to the triple junctions. The parameters $\{\alpha_i\}_{i=1,\dots,n}$ can be viewed as representing crystallographic orientations. The length of the i^{th} grain boundary is given by $l_i = x_{i+1} - x_i$. Now choose a non-negative energy density $f(\alpha)$ and define the energy

$$En(t) = \sum f(\alpha_i)(x_{i+1}(t) - x_i(t)) \tag{2.1}$$

Consider gradient flow dynamics characterized by the system of ordinary differential equations

$$\dot{x}_i = f(\alpha_i) - f(\alpha_{i-1}),\ i = 0, \dots, n. \tag{2.2}$$

The parameter α_i is prescribed for each grain boundary initially according to some random distribution and does not change during its lifetime. The velocities of the grain boundaries can be computed from the relation

$$v_i = \dot{x}_{i+1} - \dot{x}_i = f(\alpha_{i+1}) + f(\alpha_{i-1}) - 2f(\alpha_i) \tag{2.3}$$

Notice that the velocities remain constant until the moment a neighboring grain boundary collapses, at which instant a jump of the velocity occurs. Every such critical event changes the statistical state of the model through its effect on the grain boundary velocities and therefore affects further evolution of the grains. Notice that the lengths of the individual grain boundaries vary linearly between the corresponding jump events and depend entirely on the corresponding grain boundary velocities.

An important feature of the thermodynamics of grain growth is that it is dissipative for the energy during normal grain growth. At critical events, the algorithm is designed to enforce dissipation. To verify that (2.2) is also dissipative, first consider

a time t when there is no critical event. Then

$$\begin{aligned}\frac{dEn}{dt}(t) &= \sum f(\alpha_i)v_i \\ &= \sum f(\alpha_i)(f(\alpha_{i+1}) - f(\alpha_i) - f(\alpha_i) + f(\alpha_{i-1})) \\ &= \sum f(\alpha_i)(f(\alpha_{i+1}) + f(\alpha_{i-1}) - 2\sum f(\alpha_i)^2 \\ &\leqq 2\Big(\sum f(\alpha_i)^2\Big)^{\frac{1}{2}}\Big(\sum f(\alpha_i)^2\Big)^{\frac{1}{2}} - 2\sum f(\alpha_i)^2 \\ &= 0\end{aligned}$$

by periodicity and the Schwarz Inequality. This also corresponds to the fact that for any gradient flow dynamics

$$(\dot{x}_i)^2 = -\frac{\partial En}{\partial x_i}\dot{x}_i,$$

so that

$$\frac{\partial En}{\partial t} = -\sum \dot{x}_i^2 < 0.$$

Now suppose that the grain boundary $[x_c, x_{c+1}]$ vanishes at time $t = t_{crit}$ and it is the only grain boundary vanishing at t_{crit}. Then the velocity of that boundary $v_c(t) < 0,\ t < t_{crit}$, namely,

$$\frac{1}{2}(f(\alpha_{c+1}) + f(\alpha_{c-1})) < f(\alpha_c).$$

and $l_c \to 0$ for $t \to t_{crit}^-$. Now

$$En(t) > \sum_{i\neq c} f(\alpha_i)l_i,\ t < t_{crit},$$

and

$$En(t_{crit}) = \lim_{t\to t_{crit}} \sum_{i\neq c} f(\alpha_i)l_i \leqq \lim_{t\to t_{crit}} En(t).$$

Thus the model system is dissipative.

Figure 2.1 shows the behavior of velocity and length parameters of a typical grain interface in the course of the evolution. It is clear that the two quantities describing this process are the waiting times between the collision events and corresponding jump sizes of the velocities, that is there is an underlying jump process in the sense of the theory presented in earlier chapters.

From the materials science perspective, it is important to know the distributions of relative lengths, as well as grain orientations. In the most general case, we have a state space $S = \{(l, v, \alpha)\}$, where $l \in \mathbb{R}^+, v \in \mathbb{R}, \alpha \in (a, b)$.

Our goal is to obtain the set of equations describing time evolution of the joint probability density function $\rho(l, v, \alpha, t)$. These equations would completely describe the dynamics of the one-dimensional grain growth model generated by the gradient flow equation (2.2).

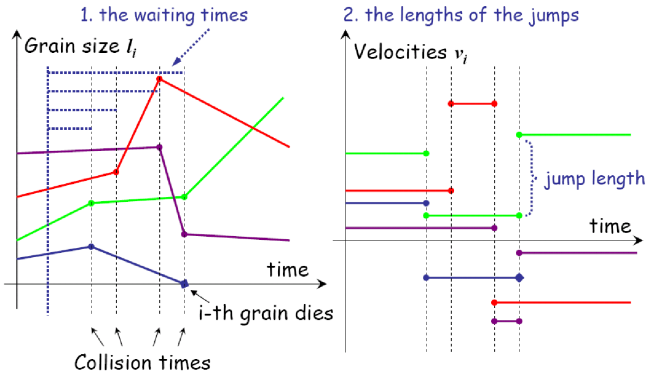

FIG. 2.1. *Schematic view of grain boundary velocities evolution.*

3. Derivation of evolution equations.

3.1. Continuous time random walk derivation of a master equation. Consider a walker making random steps in a state space X. For a walk started at x_0 at time t_0, we denote by $\bar{p}(x,t|x_0,t_0)$ the conditional probability of being found at site x at time t (site occupancy probability). We let $\bar{\phi}(x_2,t_2|x_1,t_1)$ be the conditional probability that, if the walker arrives at site x_1 at time t_1, his next step is to site x_2 and it occurs at time t_2.

Let us make the following standard assumptions on the random walk. Let the walk be homogeneous in the following sense: if the walker arrives to a point x at a time t, the probability $\phi(y,s)$ of making the next step of size y after a pause s depends on y and s, but not on x and t. Also, assume that the transition probability density ϕ can be factored into a product of a function of time and a function of step length:

$$\phi(y,s) = \mu(y)w(s).$$

Here $w(s)$ is the waiting time density and $\mu(y)$ is the step-length density defined as the marginals of the transition density ϕ. This assumption is known as a Montroll-Weiss model [8], [11].

Let $P(x,t)$ be the occupancy probability, i.e. the probability of finding the walker at the state x at time t, given that at time zero the walker was at the origin, i.e. $P(x,0) = \delta(x)$. Due to the homogeneity assumption above, if the walker arrives at x' at time t', the probability of finding him at x at time t is $P(x-x',t-t')$.

Given w, we can compute the probability that a walker arriving at a site pauses for at least time t before leaving that site:

$$\psi(t) = 1 - \int_0^t w(t')dt'.$$

The occupancy density P and the transition probability density $\phi(x,t)$ are related via a master equation that we can formally derive as follows. At time t either the walker has never left the starting site, or he has made at least one step. The probability of the former has the density $\psi(t)$ and the corresponding contribution to $P(x,t)$ is given by $\psi(t)\delta(x)$. If the walker makes one or more jumps, we may partition all possible motions over the outcome and time of occur

$$P(x,t) = \delta(x)\psi(t) + \int_0^t \int_{-\infty}^{\infty} P(x-x',t-t')\mu(x')w(t')dx'dt'. \tag{3.1}$$

Intuitively, the first term on the right-hand side above accounts for a walker who

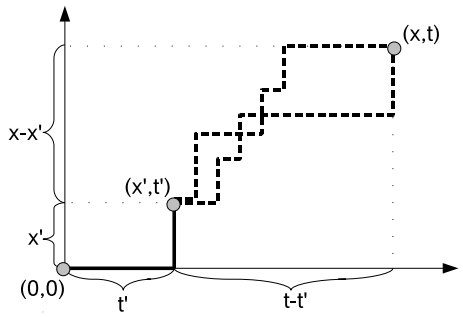

FIG. 3.1. *Random walk: partitioning over the first jump.*

fails to move from the starting position before time t elapses. The integral expresses the fact that a walker found at site x at time t after making at least one step must have made his first jump from $x_0 = 0$ to x' at some time t' and subsequently found his way to site x in remaining time $t - t'$, as shown in Figure 3.1.

3.2. Probabilistic derivation of the master equation. Let $T_i, i = 1, 2, \ldots$ be nonnegative independent and identically distributed (i.i.d) random variables with distribution $w(t)$ that model waiting times between consecutive jumps of a walker. Set $T(0) = 0$ and let

$$T(n) = \sum_{i=0}^{n} T_i$$

be the time of the n-th jump. Suppose that the jump sizes are given by the i.i.d random variables $X_i, i = 0, 1, \ldots$, with the distribution $\mu(x)$ independent of T_i. Then we can consider the random process

$$N(t) = \max\{n \geq 0 : T(n) \leq t\}$$

counting the number of jumps up to time t and define the position of the walker at time t via

$$X(t) = \sum_{i=0}^{N(t)} X_i.$$

In the previous section, we derived the evolution equation for $P(x,t) = \mathtt{P}(x < X(t) < x + dx)$ based on the CTRW formalism. Here we present an alternative derivation relying strictly on probabilistic tools.

First, by the formula of total probability,

$$\begin{aligned} P(x,t)dx &= \mathtt{P}(x < \sum_{i=0}^{N(t)} X_i < x + dx) \\ &= \sum_{k=0}^{\infty} \mathtt{P}\Big(x < \sum_{i=0}^{N(t)} X_i < x + dx \Big| N(t) = k\Big)\mathtt{P}(N(t) = k) \\ &= \delta(x)\mathtt{P}(N(t) = 0)dx + \sum_{k=1}^{\infty} \mathtt{P}\Big(x < \sum_{i=1}^{k} X_i < x + dx\Big)\mathtt{P}(N(t) = k). \end{aligned} \tag{3.2}$$

Notice that $\mathtt{P}(N(t)=0)$ is the probability a walker starting at $x=0$ and not making any moves until time t

$$\mathtt{P}(N(t)=0) = 1 - \mathtt{P}(T_0 \le t) = 1 - \int_0^t w(\tau)d\tau,$$

the survival probability, denoted as $\psi(t)$ in the previous section. Hence the contribution of this term in $P(x,t)$ has the form $\delta(x)\psi(t)$. Next, consider separately each term in the right hand side sum in (3.2). Recall from the properties of the conditional probability that for any random event B and any random variable Y with probability density f_Y,

$$P(B) = \int_{-\infty}^{\infty} \mathtt{P}(B|Y=y) f_Y(y) dy.$$

Since T_i are i.i.d. random variables with probability density w, for all $k>0$ and all $t>0$ we have

$$\mathtt{P}(N(t)=k) = \int_0^t \mathtt{P}(N(t)=k|T_1=\tau)w(\tau)d\tau = \int_0^t \mathtt{P}(N(t-\tau)=k-1)w(\tau)d\tau.$$

Similarly, due to the independence of identically distributed jumps X_i,

$$\begin{aligned}
\mathtt{P}\Big(x < \sum_{i=0}^{k} X_i < x+dx\Big) &= \int_{-\infty}^{\infty} \mathtt{P}\Big(x < \sum_{i=1}^{k} X_i < x+dx \Big| X_1 = x'\Big)\mu(x')dx' \\
&= \int_{-\infty}^{\infty} \mathtt{P}\Big(x-x' < \sum_{i=2}^{k} X_i < x-x'+dx\Big)\mu(x')dx' \\
&= \int_{-\infty}^{\infty} \mathtt{P}\Big(x-x' < \sum_{i=1}^{k-1} X_i < x-x'+dx\Big)\mu(x')dx'.
\end{aligned}$$

Therefore, from (3.2) and using Fubini theorem to justify interchange of limits of integration,

$$\begin{aligned}
&P(x,t)dx = \delta(x)\psi(t)dx + \\
&\sum_{k=1}^{\infty} \int_{-\infty}^{\infty}\int_0^t \mathtt{P}\Big(x-x' < \sum_{i=1}^{k-1} X_i < x-x'+dx\Big)\mathtt{P}(N(t-\tau)=k-1)\mu(x')w(\tau)d\tau dx' \\
&= \delta(x)\psi(t)dx + \int_{-\infty}^{\infty}\int_0^t P(x-x',t-\tau)\mu(x')w(\tau)d\tau dx'.
\end{aligned}$$

This recovers the master equation (3.1) for the probability density $P(x,t)$, that we derived earlier using intuitive arguments of the continuous time random walk theory.

3.3. Evolution equation for the random initial distribution. We gave two alternative derivations of the equation (3.1) for the probability density $P(x,t)$ with initial condition $P(x,0)=\delta(x)$. Now suppose that the initial state of the walker is not known precisely, but given by initial distribution $p(x,0)=p_0(x)$. In this situation, we can write the probability of being in state x at time t as

$$p(x,t) = \int P(x-y,t)p_0(y)dy \tag{3.3}$$

which yields

$$p(x,t) = p_0(x)\psi(t) + \int_0^t \int_{-\infty}^{\infty} p(x-x',t-t')\mu(x')w(t')dx'dt'. \tag{3.4}$$

Just as equation (3.1), equation (3.4) is called the master equation for continuous-time random walks and it holds for any walk satisfying the homogeneity and separability assumptions given above. It is worth noting that following the definition (3.3), $p(x,t)$ admits a representation $\mathtt{E}(p_0(x-X(t)))$, which corresponds to a "backward" approach in the terminology of the Markov processes. In complete analogy with the above derivations, one can derive the "forward" evolution equation for the quantity $q(x,t) = \mathtt{E}(p_0(x+X(t)))$, which satisfies

$$q(x,t) = p_0(x)\psi(t) + \int_0^t \int_{-\infty}^{\infty} q(x+x',t-t')\mu(x')w(t')dx'dt'. \tag{3.5}$$

4. Markov and non-Markov jump processes.

4.1. Generalized master equation and memory kernel. It is convenient to work with equation (3.4) in Laplace space. Indeed, denote the Laplace time variable as u and the Laplace transforms of $p(x,t)$ and $w(t)$ by $\hat{p}(x,u)$ and $\hat{w}(u)$ correspondingly. Then we arrive at

$$\hat{p}(x,u) = \frac{p_0(x)(1-\hat{w}(u))}{u} + \hat{w}(u)\int_{-\infty}^{\infty} \hat{p}(x-x',u)\mu(x')dx'. \tag{4.1}$$

We can look at this equation from a slightly different perspective, similar to that offered in [15]. After some simple algebra we can rewrite (4.1) as follows:

$$\frac{1-\hat{w}(u)}{u\hat{w}(u)}(u\hat{p}(x,u) - p_0(x)) + \hat{p}(x,u) = \int_{-\infty}^{\infty} \hat{p}(x-x',u)\mu(x')dx'$$

and let

$$\hat{\Phi}(u) = \frac{1-\hat{w}(u)}{u\hat{w}(u)}.$$

Then after changing variables inside the integral we have

$$\hat{\Phi}(u)(u\hat{p}(x,u) - p_0(x)) = \int_{-\infty}^{\infty} [\hat{p}(x-x',u) - \hat{p}(x,u)]\mu(x')dx', \tag{4.2}$$

and by taking inverse Laplace transform

$$\int_0^{\infty} \Phi(t-t')\frac{\partial}{\partial t}p(x,t')dt' = \int_{-\infty}^{\infty} [p(x-x',t) - p(x,t)]\mu(x')dx'. \tag{4.3}$$

Following [15] we call $\Phi(t)$ the "memory function" of the CTRW.

It is easy to see that (4.3) formally reduces to a differential equation if the process is Markov ("memoryless"). Then $\Phi(t) = \frac{1}{\lambda}\delta(t)$, where $\lambda = \text{const}$ and

$$\frac{\partial}{\partial t}p(x,t) = \lambda \int_{-\infty}^{\infty} [p(x-x',t) - p(x,t)]\mu(x')dx'. \tag{4.4}$$

This is equivalent to having $\hat{\Phi}(u) = \dfrac{1}{\lambda}$ and

$$\hat{w}(u) = \frac{\lambda}{u+\lambda} \text{ and } w(t) = \lambda e^{-\lambda t}.$$

In other words, in order to have a Markovian CTRW one needs to have exponentially distributed waiting times. However, we can derive a generalized master equation of the form (4.4) for a much wider class of processes. Namely, suppose

$$\hat{\Phi}(u) = \frac{1}{\lambda} u^{\beta-1}, \tag{4.5}$$

then equation (4.2) becomes

$$\frac{1}{\lambda}(u^{\beta}\hat{p}(x,u) - p_0(x)u^{\beta-1}) = \int_{-\infty}^{\infty} [p(x-x',t) - p(x,t)]\mu(x')dx', \tag{4.6}$$

which corresponds to

$$\frac{\partial^{\beta}}{\partial t^{\beta}} p(x,t) = \lambda \int_{-\infty}^{\infty} [p(x-x',t) - p(x,t)]\mu(x')dx'. \tag{4.7}$$

Here we employ the so-called Caputo fractional derivative definition

$$\frac{d^{\beta}}{dt^{\beta}} f(t) = \frac{1}{\Gamma(1-\beta)} \int_0^t \frac{f'(\tau)}{(t-\tau)^{\beta}} d\tau,$$

for which

$$\mathcal{L}\Big[\frac{d^{\beta}}{dt^{\beta}} f(t)\Big] = u^{\beta}\hat{f}(u) - u^{\beta-1}f(0).$$

The choice of $\hat{\Phi}(u)$ in (4.5) suggests the form of waiting times distribution that generalizes exponential behavior of the Markovian case. Namely,

$$\hat{w}(u) = \frac{\lambda}{u^{\beta}+\lambda},$$

which after inversion gives

$$w(t) = -\frac{d}{dt} E_{\beta}(-t^{\beta}), \tag{4.8}$$

where $E_{\beta} = \displaystyle\sum_{n=0}^{\infty} \frac{z^n}{\Gamma(\beta n + 1)}$ is the Mittag-Leffler function, which interpolates between the stretched exponential form and long-time inverse power law behavior. This is the only choice of a waiting time distribution that allows one to transform the basic CTRW equation 3.4 directly into a fractional evolution equation without a limiting procedure (see [14]). As shown in [15], we get the following asymptotic behavior for the waiting times in this case:

$$\begin{aligned} w(t) &= \frac{1}{t^{1-\beta}} \sum_{n=0}^{\infty} (-1)^n \frac{t^{\beta n}}{\Gamma(\beta n + \beta)}, && t \geq 0, \\ w(t) &\sim \frac{\sin \beta n}{\pi} \frac{\Gamma(\beta+1)}{t^{\beta+1}}, && t \to \infty. \end{aligned} \tag{4.9}$$

When $\beta = 1$ we recover the exponential waiting time behavior of the Markovian case.

Recall that in the special case of a symmetric stable Levy measure μ with index $0 < \alpha < 1$, i.e.

$$\mu(s) = \alpha s^{-\alpha-1}, \quad 0 < \alpha < 1, \quad s > 0, \tag{4.10}$$

following [9], one can define the so-called Riesz fractional derivative as

$$\frac{\partial^\alpha f}{\partial |x|^\alpha} = \frac{-1}{\Gamma(1-\alpha)} \int_0^\infty (f(x-y) - 2f(x) + f(x+y)) \alpha y^{-1-\alpha}\, dy,$$

which corresponds to the pseudo-differential operator $(-\Delta)^{\alpha/2}$ with symbol $-|k|^\alpha$, [14]. In the asymmetric case, it generalizes to

$$\frac{\partial^{\alpha_1} f}{\partial (-x)^{\alpha_1}} + \frac{\partial^{\alpha_2} f}{\partial x^{\alpha_2}}, \tag{4.11}$$

where

$$D_-^\alpha f = \frac{\partial^\alpha f}{\partial (-x)^\alpha} = \frac{-\alpha}{\Gamma(1-\alpha)} \int_0^\infty (f(x) - f(x-y)) y^{-1-\alpha}\, dy$$
$$D_+^\alpha f = \frac{\partial^\alpha f}{\partial x^\alpha}, = \frac{-\alpha}{\Gamma(1-\alpha)} \int_0^\infty (f(x+y) - f(x)) y^{-1-\alpha}\, dy$$

are the one-sided fractional derivatives of f.

In [16], it is shown that the one sided derivatives defined this way coincide with the one-sided Riemann-Liouville fractional integrals, i.e.

$$D_-^\alpha f(x) = I_-^\alpha f(x) = -\frac{d}{dx} I_-^{1-\alpha} = \frac{1}{\Gamma(\alpha)} \int_x^\infty (s-x)^{\alpha-1} f(s) ds$$
$$D_+^\alpha f(x) = I_+^\alpha f(x) = -\frac{d}{dx} I_+^{1-\alpha} = \frac{1}{\Gamma(\alpha)} \int_{-\infty}^x (x-s)^{\alpha-1} f(s) ds.$$

Notice that in the case of asymmetric stable jump sizes distribution μ, the right-hand side of the equation (4.7) is proportional to (4.11) defined above. Hence in this special case the equation (4.7) takes on the form of a fractional equation in both time and space:

$$\frac{\partial^\beta p(x,t)}{\partial^\beta t} = A_{\alpha,\beta} \frac{\partial^{\alpha_1}}{\partial (-x)^{\alpha_1}} p(x,t) + B_{\alpha,\beta} \frac{\partial^{\alpha_2}}{\partial x^{\alpha_2}} p(x,t). \tag{4.12}$$

In the case of exponential waiting times with arbitrary jump sizes, equation 4.7 coincides with the evolution equation for the Poisson jump process as developed in the theory of Levy processes (see [12],[13]).

These observations link together the theories of continuous time random walks, Levy processes and diffusion processes and justify the fact that the equation (4.7) is the most general form of the evolution equation one can get for an arbitrary space homogeneous jump process.

4.2. Asymptotic behavior and fractional kinetics. Equation (3.4) is true for any jump process expressed as a CTRW, and it depends on the forms of the model functions w and μ. We have shown how a fractional evolution equation can result from (3.4) for a special choice of waiting times (4.8) and jump sizes (4.10) densities.

In general, if the closed form of probability densities is not known, we can derive the same equation in the asymptotic limit for $t \to \infty$. The starting point for this derivation is the Montroll-Weiss equation

$$\hat{\tilde{p}}(k,u) = \frac{\tilde{p}_0(k)(1-\hat{w}(u))}{u(1-\hat{w}(u)\tilde{\mu}(k))}, \tag{4.13}$$

representing a Fourier-Laplace transform of (3.4). Here $\hat{\tilde{p}}$ denotes the Fourier-Laplace transform of p, whereas $\tilde{\mu}(k)$ and $\hat{w}(u)$ are the Fourier and Laplace transforms of $\mu(x)$ and $w(t)$ correspondingly.

If both waiting time and jump size distributions have finite variances T and Σ^2 respectively, the long-term limit of the CTRW corresponds to the Brownian motion. This easily follows from expanding Poissonian waiting times and Gaussian jump sizes in Laplace and Fourier variables correspondingly:

$$\begin{aligned} \hat{w}(u) &\sim 1 - u\tau + O(u^2), \\ \hat{\mu}(k) &\sim 1 - k^2\sigma^2 + O(k^4), \end{aligned}$$

where $\tau = T$ and $\Sigma^2 = 2\sigma^2$. Equation (4.13) then takes on the form

$$\hat{\tilde{p}}(k,u) = \frac{p_0(k)}{k + \sigma^2 u^2/\tau}$$

and by inversion converts to the classical Fokker-Planck equation ([10]). On the other hand, infinite variances corresponding to long rests and/or long jumps can result in the following expansions instead

$$\begin{aligned} \hat{w}(u) &\sim 1 - (u\tau)^\beta + O(u^\beta) \\ \tilde{\mu}(k) &\sim 1 - (k\sigma)^\alpha + O(k^\alpha). \end{aligned}$$

Substituting these expansion into (4.13), we get

$$\hat{\tilde{p}}(k,u) = \frac{u^{\beta-1}}{u^\beta + |k|^\alpha}.$$

This gives rise to the same type of fractional kinetic equation that we discussed in the previous section:

$$\frac{\partial^\beta p(x,t)}{\partial^\beta t} = D_{\alpha,\beta} \frac{\partial^\alpha p(x,t)}{\partial x^\alpha}.$$

Note that this equation has the closed form solution in the form

$$p(x,t) = \frac{1}{t^{\beta/\alpha}} W_{\alpha,\beta}\Big(\frac{x}{t^{\beta/\alpha}}\Big),$$

where $W_{\alpha,\beta}$ is the inverse Laplace transform of the Mittag-Leffler function $E_{\alpha,\beta}(z) = \sum_{j=0}^{\infty} \frac{z^j}{\Gamma(\alpha j + \beta)}$.

We remark that the fractional derivative in time introduces dependence on the past history, which brings in extra memory requirements for the corresponding numerical scheme. We will return to this point later when discussing the numerical implementation of the aforementioned fractional evolution equation.

5. Numerical results.

5.1. Simulation statistics. The first step toward a mesoscopic model is the identification of stable statistics. If the distributions behave chaotically or fail to stabilize, the analysis is significantly more complicated. To this end, we simulated the 1-dimensional system described above according to the laws of motion (2.3). The statistics of several numerical experiments for s system of 10000 grain boundaries is presented below. We refer to each grain boundary disappearance event as a simulation "step". Hence, unless there are coincident events, 10000 boundaries disappear exactly after 10000 steps.

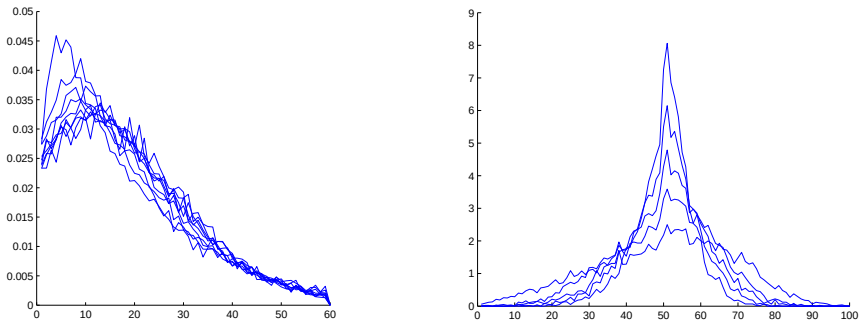

FIG. 5.1. Evolution of marginal pdf for: (a) relative lengths, (b) relative velocities for $f = (x - 0.5)^2$

Figure 5.1 shows evolution of the relative area and relative velocity distributions for the case of a single well potential. Both statistics do not change their shape in the later part of the simulation, however, their spread narrows with time, since fewer and fewer grains take part in the statistics. In this figure, the axes are scaled accordingly and we observe the stabilization of both distributions.

In Figure 5.3 we depict similar distributions for the orientation parameter α for the choice of f having either a single or triple minima. The graphs clearly show that the shapes of f and orientations distribution are inversely correlated.

Since we also want to model the evolution of these statistics at the mesoscopic level, we also need to study the waiting times and jump sizes for the grain boundary velocities, as described in Figure 2.1. Figure 5.3 shows typical behavior of these distributions. One can notice that, although the waiting times are close to being exponentially distributed, their tails might be closer to the power-law fit. As for the jump sizes, their distribution clearly depends on the form of the potential f, but remains asymmetric in both cases. Thus the observed behavior cannot be represented by the regular Gaussian distribution. Having made these observations, it becomes clear that the jump process underlying the grain growth dynamics in the 1-d case does not fit into the regular diffusion framework. However, the existence of stable statistics for both length, velocities and orientations motivates the search for a suitable statistical model for this type of dynamics.

As expected for a fractional dynamics model, our numerical experiments show that the cumulative arrivals do not behave linearly with respect to time. Figures 5.4(a) and (b) show the log-log graph of the cumulative arrivals $N(t)$ until time t for the first 4000 events and consecutive 2000 events respectively. The behavior conforms

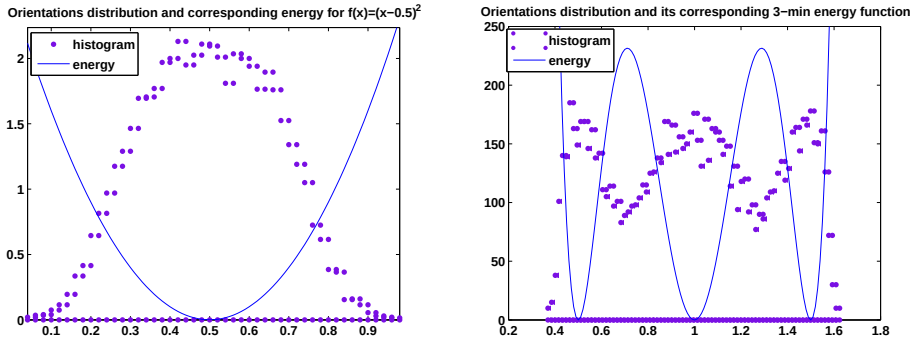

FIG. 5.2. Distribution of the orientations for (a) $f(x) = (x - 0.5)^2$, (b) $f(x) = (x - 0.5)^2(x - 1)^2(x - 1.5)^2$

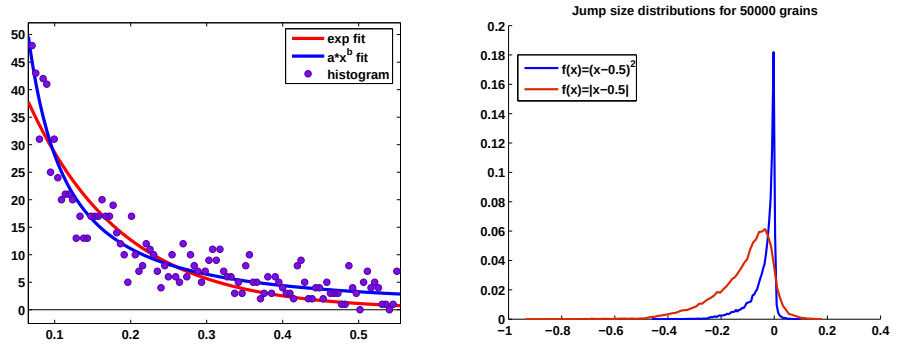

FIG. 5.3. Distribution of (a) waiting times fitted by exponential and power law curves; (b) jump sizes for $f(x) = (x - 0.5)^2$ and $f(x) = |x - 0.5|$

well with $N(t) \sim t$ in the beginning. However, when we look at $N(t) - N_0$ vs. $t - t_0$ with t_0 being the time of the 4000th arrival and $N_0 = 4000$ in Figure 5.4(b), we notice that

$$N(t) - N_0 = (t - t_0)^\beta, \text{ where } \beta \sim 0.5.$$

This points to a fact that the dynamics of the process experiences a transition from one mode to another at some critical point t_{cr} in the simulation. At the same critical time t_{cr} the stabilization of relative distributions is observed, as shown in Figure 5.1. Note that although by the time $t = t_{cr}$ almost half of the boundaries have disappeared, the absolute time elapsed from the onset of simulation remains minuscule (of the order of 10^{-2} for a 100 msec long simulation). The change in the behavior of the system can be attributed to "washing-out" of transients during the relaxation stage until it reaches the steady state. It is interesting to notice, however, that the "stable" regime corresponding to the stabilized distributions deviates significantly from regular diffusion, with $\beta = 0.5$, in contrast with the normal diffusion, where $\beta = 1$. Hence we have a case of an anomalous (sub)diffusion.

What is even more intriguing, the fractional diffusion exponent does not depend on the choice of the interfacial energy f, as shown in Figure 5.5 below. The cumulative arrival graph for all simulations experiences a transition from a $N(t) \sim t$ to a $N(t) \sim$

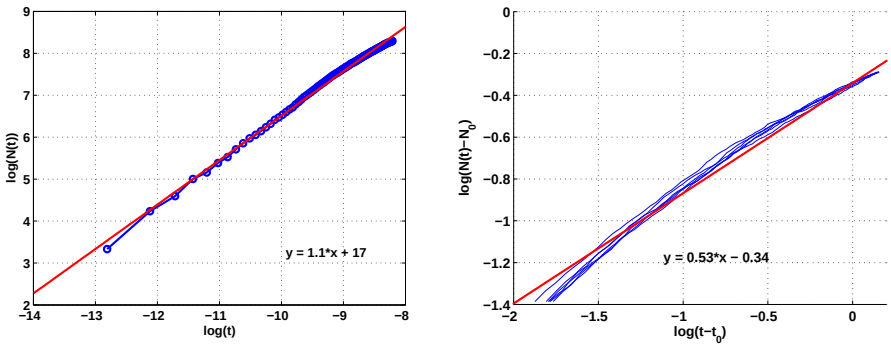

FIG. 5.4. *Cumulative arrivals vs. time in log-log scale with a linear fit for the (a) first stage of the simulation (first 4000 arrivals), (b) middle stage of the simulation (consecutive 2000 arrivals))*

$t^{1/2}$ regime around the same t_{cr} and the slope of the graph converges to the same value before and after the transition.

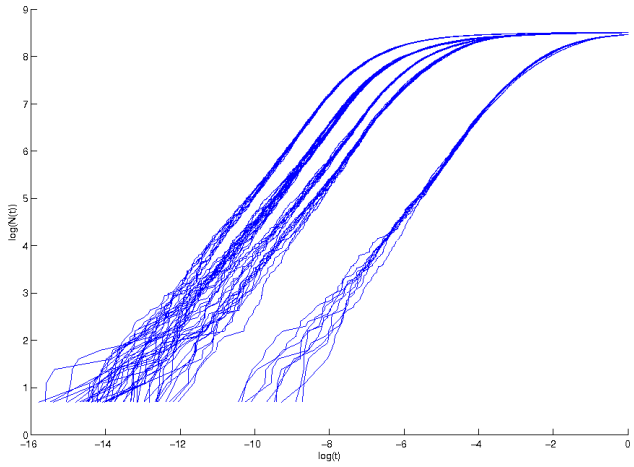

FIG. 5.5. *Cumulative arrivals $N(t)$ vs. time t in log-log scale for different choices of the potential: $f(x) = x^2, f(x) = |x-0.5|, f(x) = (x-0.5)^2, f(x) = |x-0.5|^{1/2}, f(x) = (x-0.5)^6, f(x) = (x-0.5)^2(x-1)^3$. Simulation is repeated 10 times for each potential.*

5.2. Direct simulation of fractional equation. Numerically, this equation is best solved by using Grunwald-Letnikov formulation of fractional derivative:

$$\frac{\partial^\beta f(t)}{\partial t^\beta} = \lim_{h\to 0} \frac{1}{h^\beta} \sum_{k=0}^{[t/h]} \omega_k^\beta f(t-kh), \qquad \text{where} \qquad \omega_k^{(\beta)} = (-1)^k \left(\begin{array}{c} \beta \\ k \end{array} \right).$$

Taking $\beta = 0.6$, numerical solution of the fractional Fokker-Planck equation can be obtained by using the explicit FTCS difference scheme,

$$p_j^{(m+1)} = p_j^{(m)} + S_\beta \sum_{k=0}^{m} \omega_k^{(1-\beta)} \left[p_{j-1}^{(m-k)} - 2p_j^{(m-k)} + p_{j+1}^{(m-k)} \right],$$

where $S_\beta = \frac{(\Delta t)^\beta}{(\Delta x)^2}$, which has been shown in [17] to be stable as long as

$$\Delta t \leq \frac{1}{4^{3/2-\beta}} (\Delta x)^{\frac{2}{\beta}}.$$

In the case of arbitrary $\mu(s)$, we have a modified numerical scheme

$$p_{i,j}^{(m+1)} = p_{i,j}^{(m)} + \sum_{k=0}^{m} \omega_k^{(1-\beta)} [D_\beta v_j \Delta_l p_{i,j}^{(m-k)} + S_\beta I_{i,j}^{(m-k)}], \tag{5.1}$$

where the constants take the form $S_\beta = \frac{(\Delta t)^\beta}{(\Delta l)^2}$, $D_\beta = \frac{(\Delta t)^\beta}{(\Delta l)}$.

Here we employ the following notations. The first derivative in l is computed using an upwind scheme

$$\Delta_l p_{i,j}^{(m-k)} = \frac{1}{\Delta l} \begin{cases} p_{i,j}^{(m-k)} - p_{i-1,j}^{(m-k)}, & v_j \geq 0 \\ p_{i+1,j}^{(m-k)} - p_{i,j}^{(m-k)}, & v_j < 0 \end{cases}$$

where a natural boundary condition is assumed for the part of the domain with $v > 0$. The contribution of the jump part corresponds to the following discretization of the integral:

$$I_{i,j}^{(m-k)} = \sum_{s_l : j+s_l \in [1,Nj]} \mu_l [p_{i,j+s_l}^{(m-k)} - p_{i,j}^{(m-k)}],$$

where $\mu_l = \mu(x_l)$. We determine $\mu(s)$ from the empirical jump probability density

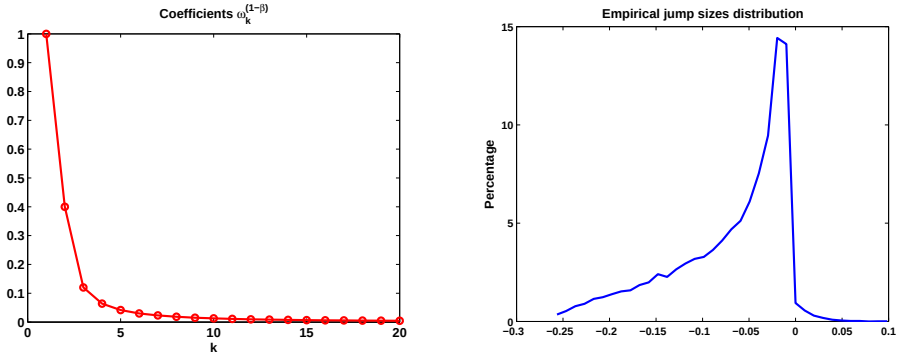

FIG. 5.6. *(a) Weights $\omega_k^{(1-\beta)}$ in Grunwald-Letnikov formulation derivative, (b)Empirical jump sizes distribution used in the simulation.*

shown in Figure 5.2 and run the model with Poisson parameter $\lambda = 1$ (4.5). Figure 5.2 shows that the results of the the FPDE simulation (right) are in reasonable agreement with simulation (left).

6. Discussion. During microstructure evolution grains coarsen by the motion of the triple junctions. The effect of topological changes (facet interchanges and disappearances) on this process is not yet understood. We propose a framework capable of describing the jump process associated with these events via a generalized continuous time random walk theory. We consider a simplified 1-dimensional model that

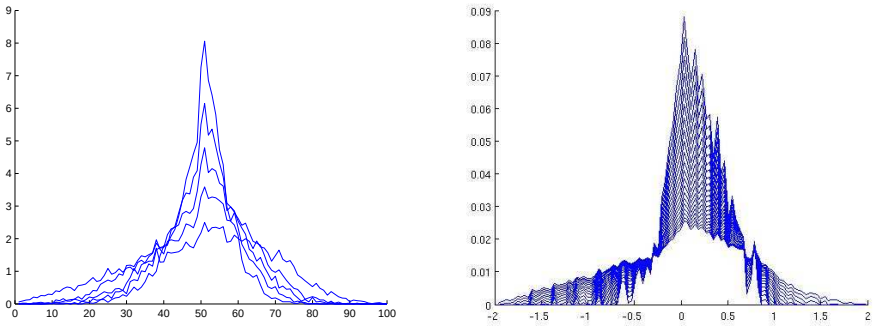

FIG. 5.7. *(a) Evolution of grain boundary velocities as collected from simulation; (b) numerical solution of the fractional equation (5.1).*

exhibits the main characteristics of the evolution of triple junctions and analyze the grain boundary distributions generated by a gradient flow dynamics imposed for this model. We show that the model possesses stable statistics for lengths, velocities and orientations and uncover a subdiffusive nature of the evolution of grain boundary velocities. By means of a continuous time random walk theory, we obtain a fractional evolution equation for grain boundary densities that shows good agreement with the statistics generated by the gradient flow dynamics in the 1-dimensional model. Although the results presented are confined to the topology of a 1-dimensional model, the form of the evolution equation will be preserved in higher-dimensions, with the only difference being the choice of distributions $w(t), \mu(s)$. Numerical implementation and testing of the higher-dimensional model are the focus of current work and will be presented in consequent publications.

7. Acknowledgment. The authors wish to thank their colleagues Eva Eggling, Katayun Barmak, Gregory Rohrer, and A. D. Rollett. Research supported by grants DMS 0405343 and DMR 0520425. DG acknowledges the support of DMS 0407361 and DK acknowledges the support of DMS 0305794.

REFERENCES

[1] Mellars, P. "Going East: New Genetic and Archaeological Perspectives on the Modern Human Colonization of Eurasia", Science, 313, 796 - 800, 2006.

[2] Kinderlehrer, D., Livshits, I., Rohrer, G.S., Ta'asan, S., and Yu, P. "Mesoscale evolution of the grain boundary character distribution, Recrystallization and Grain Growth", Materials Science Forum vols 467-470, 1063-1068, 2004.

[3] Kinderlehrer, D., Livshits, I., Manolache, F., Rollett, A. D., and Ta'asan, S., "An approach to the mesoscale simulation of grain growth, Influences of interface and dislocation behavior on microstructure evolution", (Aindow, M. et al., eds), Mat. Res. Soc. Symp. Proc. 652, Y1.5, 2001.

[4] Kinderlehrer, D., Livshits, I., and Ta'asan, S. "A variational approach to modeling and simulation of grain growth", SIAM J. Sci. Comput. Vol. 28, No. 5, pp. 16941715, 2006.

[5] S. Agmon, A. Douglis and L. Nirenberg, "Estimates near the boundary for solutions of elliptic partial differential equations satisfying general boundary conditions", II, Comm. Pure Appl. Math., 17, 3592, 1964.

[6] L. Bronsard and F. Reitich, "On three-phase boundary motion and the singular limit of a vector-valued Ginzburg-Landau equation", Arch. Rat. Mech. Anal. 124, 355379, 1993.

[7] M. Emelianenko, D. Golovaty, D. Kinderlehrer, S. Ta'asan, Grain boundary evolution: new perspectives", Center for Nonlinear Analysis, No. 06-CNA-010, 2006.

[8] Barry D. Hughes, Random Walks and Random Environments, Volume I: Random Walks, Oxford University Press, 1995.
[9] G. Zaslavsky, Hamiltonian Chaos and Fractional Dynamics, Oxford University Press, Oxford, 2005.
[10] R. Metzler, J. Klafter, The Random Walk's Guide to Anomalous Diffusion: A Fractional Dynamics Approach, Physics Reports, 339
[11] Weiss, G.H.: Aspects and Applications of the Random Walk, North Holland Press, Amsterdam, 1994.
[12] D. Applebaum, Levy Processes and Stochastic Calculus, Cambridge studies in avdanced mathematics, 93, Cambridge, 2004.
[13] M. Grigoriu, Stochastic Calculus, Applications in Science and Engineering, Birkhauser, Boston, 2002.
[14] R. Gorenflo, A. Vivoli, F. Mainardi, "Discrete and Continuous Random Walk Models for Space-time Fractional Derivatives", J. Math. Sci., **vol. 132**, No. 5, 2006.
[15] F. Mainardi et al, Fractional calculus and continuous-time finance II: the waiting-time distribution, Physica A, 287, p.468-481, 2000.
[16] R. Gorenflo, F. Mainardi, "Essentials of Fractional Calculus", MaPhySto Center preprint, 2000.
[17] S.B. Yuste, L. Acedo, "An explicit finite difference method and a new Von Neumann-type stability analysis for fractional diffusion equation", SIAM J. Numer. Anal., Vol.42, No.5, p. 1862-1974, 2005.